Effects of the Eukaryotic Pore-Forming Cytolysin Equinatoxin II on Lipid Membranes and the Role of Sphingomyelin

Boyan B. Bonev,* Yuen-Han Lam,† Gregor Anderluh,‡ Anthony Watts,* Raymond S. Norton,§ and Frances Separovic†

*Biomembrane Structure Unit, Department of Biochemistry, University of Oxford, Oxford OX1 3QU, UK; †School of Chemistry, University of Melbourne, Victoria 3010, Australia; ‡Department of Biology, Biotechnical Faculty, University of Ljubljana, Vecna pot 111, 1000 Ljubljana, Slovenia; and §Biomolecular Research Institute, 343 Royal Parade, Parkville 3052, Australia

ABSTRACT Equinatoxin II (EqtII), a protein toxin from the sea anemone *Actinia equina*, readily creates pores in sphingomyelin-containing lipid membranes. The perturbation by EqtII of model lipid membranes composed of dimyristoylphosphatidylcholine and sphingomyelin (10 mol %) was investigated using wideline phosphorus-31 and deuterium NMR. The preferential interaction between EqtII (0.1 and 0.4 mol %) and the individual bilayer lipids was studied by ^{31}P magic angle spinning NMR, and toxin-induced changes in bilayer morphology were examined by freeze-fracture electron microscopy. Both NMR and EM showed the formation of an additional lipid phase in sphingomyelin-containing mixed lipid multilamellar suspensions with 0.4 mol % EqtII. The new toxin-induced phase consisted of small unilamellar vesicles 20–40 nm in diameter. Deuterium NMR showed that the new lipid phase contains both dimyristoylphosphatidylcholine and sphingomyelin. Solid-state ^{31}P NMR showed an increase in spin-lattice and a decrease in spin-spin relaxation times in mixed-lipid model membranes in the presence of EqtII, consistent with an increase in the intensity of low frequency motions. The ^{2}H and ^{31}P spectral intensity distributions confirmed a change in lipid mobility and showed the creation of an isotropic lipid phase, which was identified as the small vesicle structures visible by electron microscopy in the EqtII-lipid suspensions. The toxin appears to enhance slow motions in the membrane lipids and destabilize the membrane. This effect was greatly enhanced in sphingomyelin-containing mixed lipid membranes compared with pure phosphatidylcholine bilayers, suggesting a preferential interaction between the toxin and bilayer sphingomyelin.

INTRODUCTION

Pore-forming peptides and proteins from the defense systems of higher organisms, as well as many bacterial toxins, are usually water-soluble molecules, which bind to their target membranes then self-associate and translocate across the lipid bilayer into transient or stable lytic pores (Dempsey, 1990; Menestrina et al., 1994; Broekaert et al., 1997; Minn et al., 1997, Gouaux, 1997; Anderluh and Macek, 2002). The action of such toxins can be investigated directly by studying the changes they induce in the target membranes, as well as the role the target lipid membrane constituents play in the process of cell lysis. In some cases the presence of specific molecular species in the target membrane is required for membrane recognition before pore-formation. One such example includes the class of cholesterol-binding toxins, which are highly hemolytic to mammalian cells while providing self-immunity to the cholesterol-free bacterial membranes of the source organisms (Bonev et al., 2001a).

Equinatoxin II (EqtII) is a 179-residue, 19.8-kDa cytolysin isolated from the Mediterranean anemone *Actinia equina* L. (Macek and Lebez, 1988). Analysis of the amino acid (Simpson et al., 1990; Belmonte et al., 1994) and nucleotide sequences of EqtII and other actinoporins (Anderluh et al., 1996; Pungercar et al., 1997) showed no obvious similarity to other pore-forming proteins and they appear to constitute a novel family. These toxins are characterized by a high pI, a molecular mass of ~20 kDa, affinity for sphingomyelin (SM) and permeabilizing activity in model lipid and cell membranes (Zorec et al., 1990; Belmonte et al., 1993; Macek et al., 1994). Recently the crystal (Athanasiadis et al., 2001) and solution (Zhang et al., 2000; Hinds et al, 2002) structures of EqtII have been reported. Although these structures provide clues as to which regions of EqtII might interact with lipid membranes and undergo conformational changes, no direct experimental evidence was obtained concerning the conformational changes EqtII undergoes in reaching its oligomeric state, or during its incorporation into the target membrane.

EqtII-induced pore formation appears to involve the monomer binding to the membrane (Macek et al., 1995), followed by insertion and noncovalent oligomerization of monomers into a pore with an effective inner hydrodynamic radius of 1.1 nm (Belmonte et al., 1993). Analysis of the dose-response relationship for EqtII and another SM-preferring cytolytic toxin, sticholysin I, produces Hill coefficients of 3–4 (Michaels, 1979; Varanda and Finkelstein, 1980; Belmonte et al., 1993). Cross-linking experiments on membranes (Belmonte et al., 1993) as well as

Submitted February 27, 2002, and accepted for publication December 2, 2002.

Address reprint requests to Frances Separovic, School of Chemistry, University of Melbourne, VIC 3010, Australia. Tel.: 61-3-8344-6464; Fax: 61-3-9347-5180; E-mail: fs@unimelb.edu.au.

Raymond S. Norton's present address is The Walter and Eliza Hall Institute of Medical Research, NMR Laboratory, 381 Royal Parade, Parkville 3052, Australia.

Boyan B. Bonev's present address is School of Biomedical Sciences, University of Nottingham, Nottingham, NG7 2UH, UK.

0006-3495/03/04/2382/11 $2.00

kinetic measurements with sticholysin I (Tejuca et al., 1996) suggest the existence of a trimer or tetramer in the structure of the functional pore.

In principle, at least two steps are involved in formation of the EqtII pore, initial binding of monomers to the membranes and subsequent oligomerization into a functional pore. However, it has been shown that the most abundant form of the toxin on the membrane is the monomer and that the fraction of toxin associated in pores is actually small (Belmonte et al., 1993; Tejuca et al., 1996). At lipid/toxin molar ratios of 400, ~80% of the protein was bound (Anderluh et al., 1999), with 100–200 EqtII monomers bound per unilamellar vesicle of ~100-nm diameter. Interestingly, the number of pores determined from permeabilization experiments was never higher than 2–3 per vesicle at a total lipid/toxin ratio of 10 and would certainly be less at a lipid/toxin ratio of 400 (Macek et al., 1995; Tejuca et al., 1996). This clearly indicates that most of the toxin is not in an oligomeric form. Hence, NMR studies of the interaction of EqtII with lipid bilayers are likely to report on lipid-protein interactions rather than pore formation.

The nature of the interaction between EqtII and the lipids in bilayer membranes and, in particular, the specific role of sphingomyelin in pore formation are poorly understood (Bernheimer and Avigad, 1976; Tejuca et al., 1996). The insertion of EqtII into phosphatidylcholine monolayers is optimal when the SM content is 50% of the phospholipid (Caaveiro et al., 2001), although one biological target of EqtII, the red blood cell membrane, contains between 5 and 30 mol % SM.

The interaction of membrane water-soluble proteins with specific lipids in model membranes has been investigated previously using solid-state NMR techniques (Pinheiro and Watts, 1994; Carbone and Macdonald, 1996; Bonev et al., 2000a). Here we apply similar solid-state NMR methods to study the interaction between EqtII and sphingomyelin-containing bilayer lipid membranes, with the aim of elucidating the nature of the lipid-toxin interaction and its role in the pore-forming mechanism.

MATERIALS AND METHODS

Equinatoxin II

Equinatoxin II was prepared from sea anemone extracts as described by Macek and Lebez (1988). Briefly, sea anemones were gently squeezed and the released liquid was collected. The obtained extracts were fractionated by acetone precipitation. The precipitate obtained after final concentration in 80% acetone was dissolved in 10 mM acetic acid and applied to a Sephadex G50 (Sigma, St Louis, MO) column. Active fractions were pooled and applied to a CM-cellulose (Sigma) column. Bound toxin was eluted using a salt gradient. Active fractions were dialyzed three times against water and the toxin was lyophilized. Lyophilized toxin was dissolved in a small volume of distilled water and dialyzed a further three times against 5 L of water to remove traces of salt and buffer. EqtII was lyophilized again and stored as a dry powder at −20°C until use.

Lipids

Brain sphingomyelin (Avanti Polar Lipids, Inc., Alabaster, AL) was used as shipped without further purification. Chain perdeuterated dimyristoylphosphatidylcholine (DMPC-d_{54}) was synthesized from perdeuterated myristic acid by acylation of glycerophosphocholine (Sigma), as described previously (Bonev and Morrow, 1997). The final product was purified on a silica gel, mesh 60, liquid chromatography column and eluted with a 65:25:5 mixture of chloroform/methanol/28% ammonia. The lipid was found to migrate as a single spot under thin layer chromatography. All NMR experiments were repeated using commercially available DMPC-d_{54} (Avanti Polar Lipids Inc.) and similar results were obtained.

Sample Preparation

For sample preparation, lipids (DMPC or 10 DMPC:1 SM mole ratio) were mixed in a chloroform/methanol (2:1) system 10 mg/mL in a round-bottom flask. The solvent was subsequently removed using a rotary evaporator and the lipid mixtures were dried under high vacuum for 3–5 h. Lyophilized EqtII was dissolved in water at a concentration of 2 mg/ml (pH ~6.5) and appropriate amounts used to give the desired toxin-lipid ratio (e.g. 1000 DMPC:100 SM:1 EqtII or 1000 DMPC:1 EqtII). Approximately 30 mg of the lipid mixtures were hydrated in 1.0 mL of toxin in deionised water. Each sample was subsequently put through five cycles of rapid freezing in liquid nitrogen and equilibrating at 50°C. The multilamellar vesicle (MLV) suspensions were then concentrated in a Beckman bench top centrifuge (20,000 rpm, 20 min, 4°C). The pellet was loaded directly into 4 mm or 5 mm NMR zirconia rotors for the Magic Angle Spinning (MAS) experiments or 5 mm Pyrex NMR tubes for static wideline measurements.

NMR spectroscopy

Phosphorus-31 wideline and MAS NMR measurements were carried out on CMX Infinity 200 and 500 spectrometers (Chemagnetics, Varian, Palo Alto, CA) at proton frequencies of 200 and 500 MHz, respectively. Typically 20 μmol of phospholipid dispersions were packed in 4-mm rotors for use with either a 200 MHz CP probe (Bruker Spectrospin, Etlingen, Germany) or a 500 MHz Apex (Chemagnetics) CP MAS probe. A single ^{31}P 90° pulse was used for excitation, with broadband decoupling at the proton frequency during acquisition. The 90° pulse length was 4 μs, and the strength of the proton decoupling field was 20 kHz. The dwell time was 20 μs and 2048 points were collected in each experiment. Between 300 and 3000 transients were averaged for each free induction decay during magic angle spinning experiments and between 5000 and 10000 during wideline experiments, with a 5 s delay (exceeding $5 \times T_1$) between acquisitions in all cases, where T_1 is the longitudinal relaxation time. The sample rotation speed was maintained at 12 kHz during acquisition of the MAS spectra and the temperature was 40°C.

Variable-temperature experiments and ^{31}P relaxation measurements were carried out on a Varian Inova 300 NMR spectrometer equipped with a Doty MAS probe (Doty Scientific Inc., Columbia, SC) operating at 121.5 MHz for ^{31}P, as well as on the abovementioned CMX Infinity 200 spectrometer. The following conditions were used: sweep width 62.5 kHz, 90° pulse 3.2 μs, recycle time 2 s, number of transients 2400–4196, line broadening 100 Hz and a temperature range of 25–50°C with 5°C intervals. The spin-lattice relaxation time, T_1, was measured using the inversion recovery ($\pi - \tau - \pi/2$) pulse sequence, with τ values between 0.005 and 8.0 s. Spin-spin relaxation time, T_2, measurements were made using a spin-echo experiment ($\pi/2 - \tau - \pi$) with τ values between 0.1 and 5 ms to observe the decay in spectral intensity. Duplicate experiments were run and relaxation times determined by fitting a single exponential to a plot of signal intensity against the delay time τ (Homans, 1992). Errors estimated from the residual spectral intensity during spectral simulations were less than ±2.5%.

In the high resolution ^{31}P MAS experiments, described here, the spectral density function, $J(\omega_0)$, has a Lorentzian shape:

$$J(\omega_0) = \tau_c/(1 + \omega_0^2\tau_c^2).$$

The spin-lattice relaxation rate, $1/T_1$, which is proportional to $J(\omega_0)$ (Haeberlen and Waugh, 1969), is highest when the characteristic correlation time of the dominant molecular motions equals the inverse of the Larmor frequency, $\tau_c = 1/\omega_0$. Shifts in the T_1 minimum, are, therefore, indicative of changes in the rate of molecular motions. Also, an order of magnitude estimate of τ_c can be obtained ($\sim$10 ns for ^{31}P ω_0 of 81 MHz).

Deuterium NMR experiments were performed using a Chemagnetics Infinity 400 spectrometer at proton frequency of 398 MHz. A quadrupole echo sequence ($\pi/2 - \tau - \pi/2 - \tau$ – acquisition) (Davis et al., 1976) was used with interpulse delay τ of 40 μs. The 90° pulse length was 4 μs and the repetition time was 0.5 s. Between 1024 and 96000 transients were averaged per free induction decay.

The quadrupole splitting, observed from each deuterated methylene segment, is related to the mean orientational order parameter of this segment as follows:

$$\Delta\nu_Q = 3/4(e^2qQ/h) \times S_{CD}$$

and is a sensitive probe for detecting changes in the overall order of the phospholipids chains. The quantity in brackets is the carbon-deuterium quadrupole coupling constant, equal to 167 kHz for C–D bonds (Seelig, 1977). Variable temperature ^{2}H spectra were acquired between 25 and 50°C with a 5°C interval using a Varian Inova 300 NMR spectrometer equipped with a Doty 5-mm probe (Doty Scientific Inc.). The ^{2}H operating frequency was 46.1 MHz and the following parameters were used: sweep width 180 kHz, $\pi/2$ pulse 5.6 μs, recycle time 0.3 s, τ 40 μs, number of transients 3200–8096, and line broadening 50 Hz.

Electron microscopy

Samples of DMPC/SM/EqtII were equilibrated at room temperature and quenched for freeze-fracture by rapid ($\sim 10^4$–10^5 °C/s) immersion into liquid butane (Severs et al., 1995; Shotton and Severs, 1995). The immobilized frozen samples were fractured at −100°C, Pt shadowed at angles of 45° and a carbon film was subsequently applied perpendicular to the fracture plane in a Balzers (Liechtenstein) freeze-etching apparatus. Residual sample was removed using consecutive washes in potassium hypochlorate, water, and methanol. The carbon-platinum replicas were transferred from a finishing water bath onto copper electron microscope grids. Micrographs were acquired using a Phillips (Netherlands) CM120 transmission electron microscope at 100 kV cathode voltage.

RESULTS

Phosphorus-31 wideline NMR

The effect of EqtII on phospholipid phase behavior was investigated using wideline ^{31}P NMR. Spectra from DMPC and from a DMPC-SM (10:1 mol ratio) mixture in water at 25 and 40°C without EqtII are shown in Fig. 1, *a* and *f*, and Fig 1, *b* and *g*, respectively. These spectra are very similar and consist of powder distributions dominated by the effective chemical shift anisotropy (CSA) of the lipid phosphates. The observed spectral width of $\sim$42 to 48 ppm reflects partial motional averaging of the ^{31}P CSA due to fast axial rotation of the phospholipid molecules, which is characteristic of the fluid bilayer phase. A single powder pattern is observed in each case, which suggests that the lipid

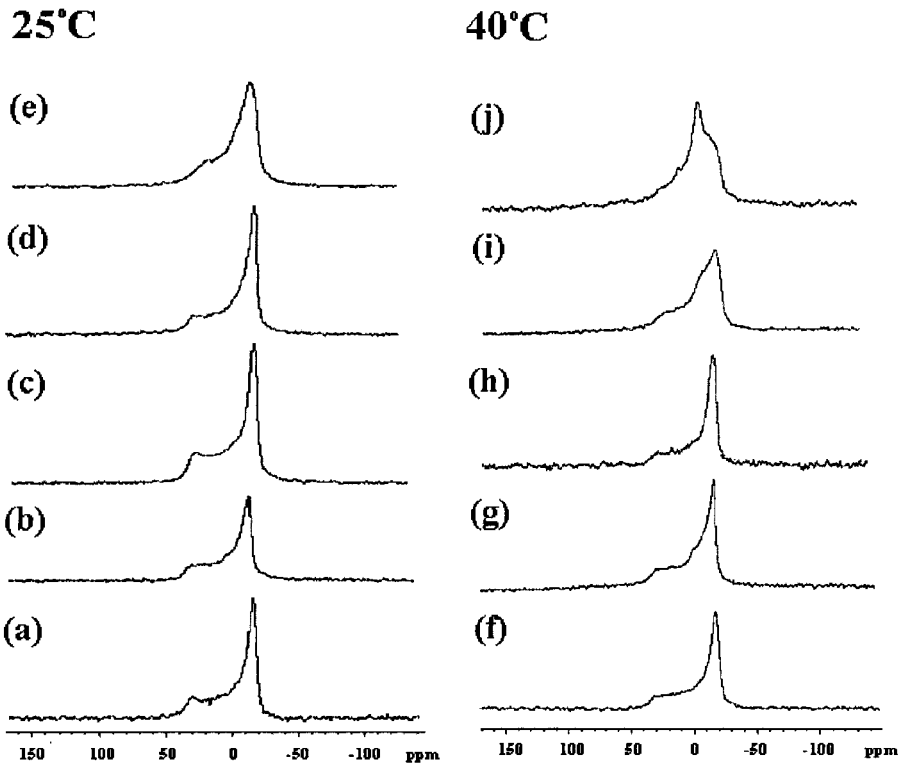

FIGURE 1 Phosphorus-31 wideline NMR spectra from hydrated DMPC/SM/EqtII suspensions at 25°C: (*a*) DMPC; (*b*) 1000 DMPC: 1 EqtII; (*c*) 1000 DMPC: 100 SM; (*d*) 1000 DMPC: 100 SM: 1 EqtII; and (*e*) 1000 DMPC: 100 SM: 4 EqtII; and at 40°C: (*f*) DMPC; (*g*) 1000 DMPC: 1 EqtII; (*h*) 1000 DMPC: 100 SM; (*i*) 1000 DMPC: 100 SM: 1 EqtII; and (*j*) 1000 DMPC: 100 SM: 4 EqtII. The acquisition parameters are described in Materials and Methods.

species are well mixed in the bilayer and the average size of the lipid aggregates exceeds 1 μm. This is a good indication that the sample is, indeed, an MLV dispersion (Seelig, 1978).

Addition of either 10% SM (Fig. 1 *b*) or 0.1% EqtII (Fig. 1 *c*) to pure DMPC bilayers resulted in a decrease of the effective phosphorus CSA from ~47 ppm for pure DMPC to ~43 ppm in both cases. The effect of both additives, therefore, amounts to a slight perturbation in the packing of the bilayer phospholipids. After addition of both 10% SM and 0.1% EqtII at 25°C (Fig. 1 *d*), however, the observed effective CSA was ~47 ppm, which was comparable to that of pure DMPC at 25°C. The action of 0.1% EqtII on the mixed lipid bilayer system at 40°C (Fig. 1 *i*) led to the formation of an additional lipid phase.

The increase in the overall effective ^{31}P CSA of the mixed lipid bilayer phosphates (DMPC/SM/EqtII, 1000:100:1 molar parts) at 25°C is close to that observed in a pure DMPC bilayer. This combined effect of EqtII and SM is consistent with the formation of SM-rich/EqtII lateral domains, surrounded by a DMPC-rich, SM-depleted lateral bilayer phase. This phase is in thermodynamic equilibrium with the SM-rich proteolipid bilayer domains and its spectral features dominate the intensity distribution in the spectrum of Fig. 1 *d*.

Spectra of DMPC/SM (10:1 molar parts) and 0.4% EqtII at both 25°C and 40°C are characterized by a dramatic increase in the isotropic ^{31}P line width, seen in the poorly defined 0 and 90° edges of the ^{31}P wideline NMR spectra (Fig. 1, *e* and *j*), and an overall shape of the wideline intensity distribution which is usually associated with the formation of a gel phase (Fig. 1, *e* and *j*) (Seelig, 1978). In addition, at 40°C the presence of 0.4% EqtII leads to the formation of an additional phase, which is observed in the spectral feature at 0 ppm (Fig. 1 *j*). The phospholipid structures in this phase undergo fast isotropic motions, which average out completely the phosphate CSA. The spectral contribution from the new phase was greater in the presence of 0.4% than 0.1% EqtII (cf. Fig. 1, *j* and *i*, respectively).

Deuterium wideline NMR

In a set of experiments, parallel to the wideline ^{31}P measurements described above, chain perdeuterated DMPC was used to investigate the effect of EqtII on chain order and mobility. The spectra from DMPC in the fluid bilayer phase (Fig. 2, *a* and *f*) consist of superimposed powder doublets with quadrupole splittings not exceeding 33.4 kHz at 25°C and 27.8 kHz at 40°C. After addition of 0.1 molar % EqtII the observed maximum quadrupole splitting was reduced to ~29.6 kHz at 25°C and 25.9 kHz at 40°C (Table 1). This reduction in lipid chain order most likely reflects incor-

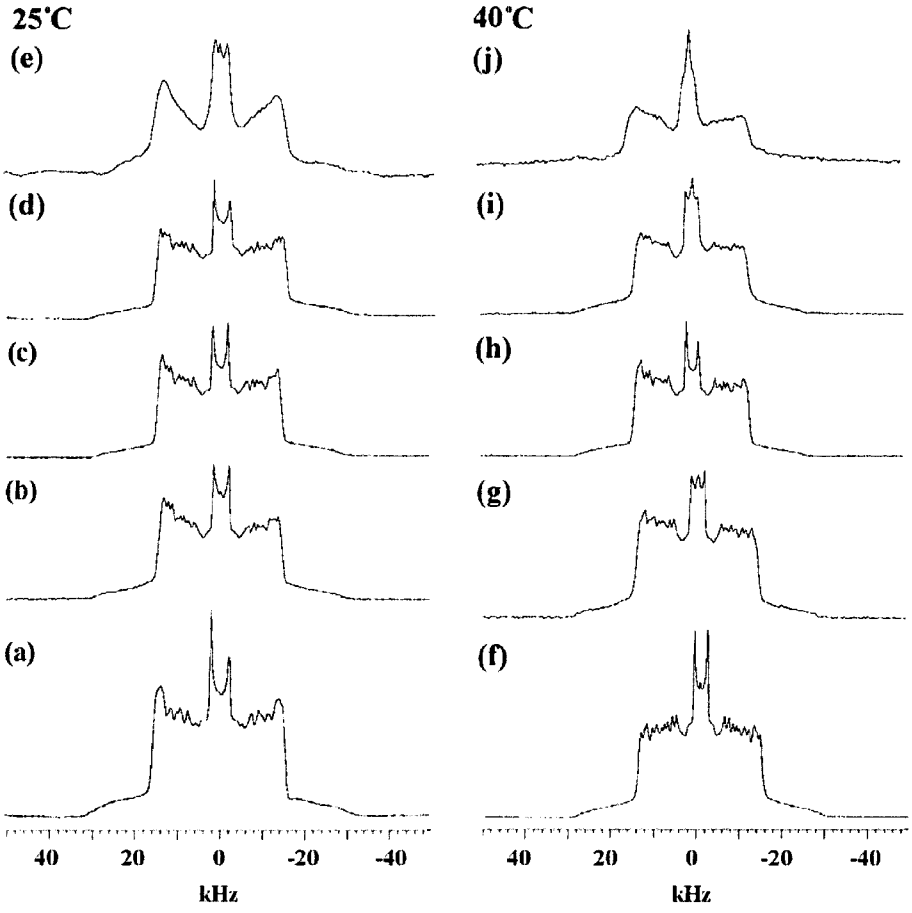

FIGURE 2 Deuterium wideline NMR spectra from hydrated DMPC/SM/EqtII suspensions at 25°C: (*a*) DMPC; (*b*) 1000 DMPC: 1 EqtII; (*c*) 1000 DMPC: 100 SM; (*d*) 1000 DMPC: 100 SM: 1 EqtII; and (*e*) 1000 DMPC: 100 SM: 4 EqtII; and at 40°C: (*f*) DMPC; (*g*) 1000 DMPC: 1 EqtII; (*h*) 1000 DMPC: 100 SM; (*i*) 1000 DMPC: 100 SM: 1 EqtII; and (*j*) 1000 DMPC: 100 SM: 4 EqtII. The acquisition parameters are described in Materials and Methods.

TABLE 1 Phosphorus-31 MAS NMR transverse relaxation times and maximum deuterium quadrupole splittings from pure and mixed lipid membranes with and without EqtII

	^{31}P MAS $T_2 \pm 0.15$ [ms]		^{2}H static, $\Delta\nu_Q \pm 0.2$ [kHz]	
Sample (mol:mol)	25°C	40°C	25°C	40°C
DMPC	3.7 ms	3.5 ms	33.4 kHz	27.8 kHz
1000 DMPC: 100 SM	2.7 ms	3.6 ms	29.6 kHz	25.9 kHz
1000 DMPC: 1 EqtII	2.8 ms	3.5 ms	29.2 kHz	26.8 kHz
1000 DMPC: 100 SM: 1 EqtII	1.7 ms	3.4 ms	29.7 kHz	26.6 kHz
1000 DMPC: 100 SM: 4 EqtII	1.1 ms	3.8 ms	n/d*	26.8 kHz

*Spectral intensity distribution does not reflect purely axially-symmetric lipid motions and $\Delta\nu_Q$ cannot be determined in a simple way.

poration of toxin. Since the character of the spectra appears to remain basically unchanged there is no evidence of any specific interaction between the toxin and DMPC-d_{54}.

The mixed lipid system, consisting of 10:1 molar parts DMPC-d_{54}/SM, was in the fluid bilayer phase at both 25 and 40°C. The observed maximum deuterium quadrupole splittings (Fig. 2, *c* and *h*) were 29.1 kHz at 25°C and 26.8 kHz at 40°C. The slight reduction in overall chain order can be attributed to a perturbation of DMPC-d_{54} chain packing by SM.

The effect of 0.1 molar % EqtII on the PC/SM lipid mixture was manifested in a slightly different manner in the deuterium spectra at 25 and 40°C. At 25°C the presence of toxin led to a reduction in the deuterium spectral width from 33.4 to 29.7 kHz. Interestingly, the overall width was slightly greater than that from DMPC-d_{54} mixtures with either SM or EqtII (29.6 and 29.1 kHz, respectively).

At 40°C a new phase was formed, the existence of which was manifested in the deuterium NMR spectra as an isotropic line at zero quadrupole splitting (cf. ^{31}P wideline, above and EM results, below). The overall spectral width was reduced to 26.6 kHz in comparison with pure DMPC-d_{54} (27.8 kHz). The maximum quadrupole splitting fell between that from DMPC-d_{54}/SM (25.9 kHz) and DMPC-d_{54}/EqtII (26.8 kHz), which suggests the mixed effect of both additives on the DMPC-d_{54} reporter molecules.

One possible explanation for the spectral features in Fig. 2, *d* and *i* is that the temperature range of the PC/SM fluid-gel coexistence region is extended toward higher temperatures by the presence of EqtII. At 25°C the fluid bilayer component is within this region and consists of two sub-phases, a fluid DMPC-d_{54}-rich sub-phase and an SM-rich sub-phase. The maximum spectral width is dominated by the order in the DMPC-d_{54}-rich sub-phase, as it sequesters preferentially the reporter lipid. At 40°C the bulk bilayer lipid is in the fluid phase and such demixing does not take place. This effect of EqtII was confirmed by differential scanning calorimetry, which showed an elevation of the main gel-fluid lipid phase transition from 20°C for the deuterated DMPC-d_{54} sample to 21°C and a slight broadening with 10% SM or 0.1% EqtII (data not shown). When EqtII was added to DMPC with 10% SM, the phase transition broadened significantly and, for the 1000 DMPC: 100 SM: 4 EqtII sample, extended over the range 20–35°C.

This EqtII-induced lateral domain formation and phase separation is enhanced by increasing the toxin concentration to 0.4 mol %. At 25°C this results in a shift of the lipid phase coexistence in favor of the motionally restricted low temperature phase and an enhanced transverse relaxation of the chain methylene deuterons (Fig. 2 *e*). In addition, a small fraction of the lipid phase with isotropic spectral features is also formed. At 40°C the relative fraction of this new phase is strongly enhanced, as is the transverse relaxation rate R_2 (Fig. 2 *j*). The deuterium T_2 also appears to depend on the methylene position within the acyl chains (cf. Bonev and Morrow, 1996). Two phenomena could be taking place simultaneously: 1), lateral phase separation within the bilayer, due to segregation of SM by EqtII, and 2), phase separation, resulting from withdrawal of lipid material from the bilayer into SUVs or similar proteolipid structures by EqtII. The first effect would manifest itself in changes of the observed maximum quadrupole splitting, and the second would result in the presence of an isotropic peak.

Electron Microscopy

Freeze-fracture electron micrographs from DMPC/SM/EqtII (mole ratio 1000:100:4) MLVs, flash-frozen from 30°C, are shown in Fig. 3. The most prominent features in the micrographs are 300 to 500 nm MLVs frozen from the rippled $P_{\beta'}$ phase, which coexist with a large number of very small, most probably unilamellar, vesicles with diameter varying between 20 and 40 nm. These structures were not present in DMPC/EqtII or DMPC/SM samples (data not shown). The multilamellar character of the primary lipid population is observed in multiple jagged edges traversing the fractured faces of the MLVs (Fig. 3 *a*). The entire surface of the MLVs is rippled with periodicity of ~70 Å, which is characteristic of the $P_{\beta'}$ phase (this effect was seen also in the DMPC/SM and DMPC/EqtII samples). One interesting feature of the MLV surface topography is the unusually irregular relief. A large number of smaller diameter, spherical structures appear trapped in the interior of larger diameter vesicles (Fig. 3 *c*). Imprints from objects of the same size as the small lipid structures are visible on the surfaces of the MLVs (Fig. 3 *b*). The cross section of the MLV walls appears swollen, unlike the regular and periodic lamellar packing observed in pure lipid systems (not shown). A number of small vesicles appear to bud off from the MLV surfaces (Fig. 3 *c*); and imprints from vesicles removed by fracture are visible, Fig. 3 *b*). The small unilamellar lipid population most likely originates from the MLVs, the lamellae of which have been destabilized by the toxin. Lipid material has been withdrawn from the low curvature MLV surfaces into highly curved proteolipid structures in a similar manner to the changes in the lipid bilayer observed dur-

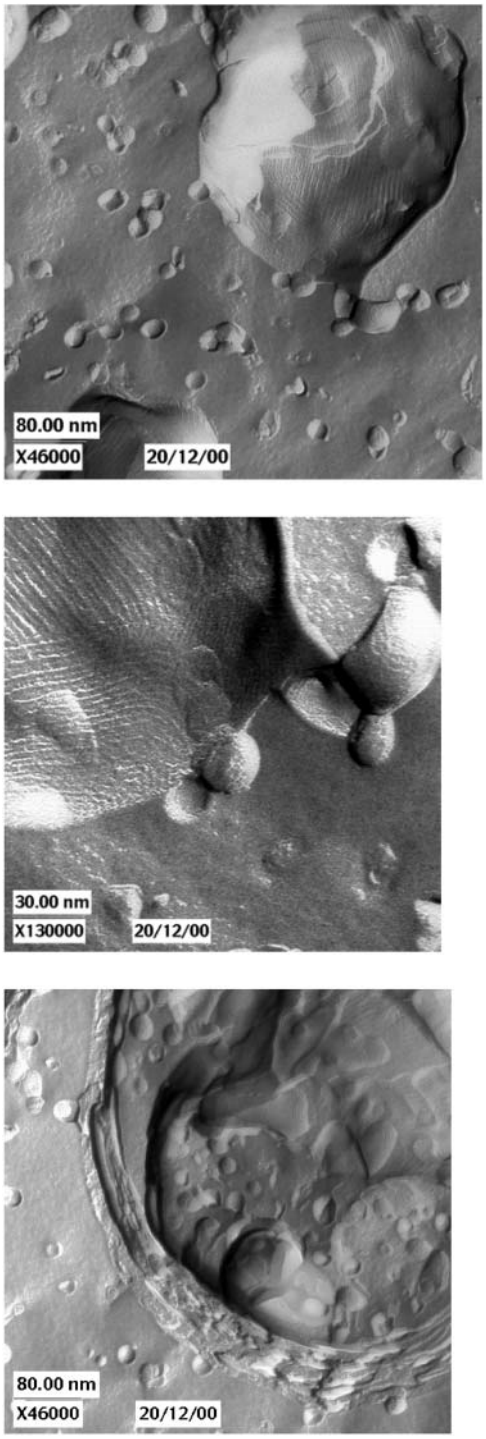

FIGURE 3 Freeze-fracture electron micrographs of hydrated DMPC/SM/EqtII (1000:100:4 mol ratio) suspension (from top to bottom): (*a*) 46,000× magnification; (*b*) 130,000× magnification; and (*c*) another view at 46,000× magnification.

ing membrane perturbation by pneumolysin (Bonev et al., 2000b, 2001a). The presence of MLVs was also reflected in the observed wideline ^{31}P-powder patterns and ^{2}H- quadrupolar splittings (Davis et al., 1976), while the SUV population gave rise to the isotropic lines seen at ~0 ppm in both ^{31}P and ^{2}H NMR wideline spectra (Figs. 1 and 2).

A close examination of the small vesicle surfaces reveals the presence of an unusual soccer ball pattern, distinctly different from the 70-Å ripple on the MLV surfaces. This pattern reflects the different lipid and protein packing on the surface of the small lipidic particles. A sucrose density gradient (0–50%) centrifugation revealed the presence of an extra band in the DMPC/SM/EqtII sample in addition to the major fraction, which appeared at the same position as the MLV band of the control DMPC/SM sample (1.105 gm/mL density). The additional layer in the EqtII-containing sample was at 1.030 gm/mL, corresponding approximately to the expected position of protein-free SUV (Watts et al., 1978). Interestingly, similar small lipid structures are observed by the action of EqtII on V-79 cells (Batista and Jezernik, 1992).

Phosphorus-31 MAS NMR

Changes in the individual lipid species within the bilayer caused by EqtII can be monitored simultaneously by using high-resolution solid-state ^{31}P MAS NMR, which allows for each lipid component to be resolved by its isotropic chemical shift (Pinheiro and Watts, 1994). Such changes have been observed previously during the interaction of other peptides and proteins with lipid membranes (Pinheiro and Watts, 1994; Carbone and Macdonald, 1996; Bonev et al., 2000a, 2001a).

The ^{31}P MAS NMR spectrum from a lipid mixture of DMPC/SM in a 10:1 mole ratio after a single-pulse excitation is shown in Fig. 4 *a*. The individual spectral contributions from PC at −0.87 ppm and SM at −0.24 ppm are well resolved and their spectral intensities reflect the molar ratio of each lipid in the mixture. Two high-resolution ^{31}P MAS NMR spectra were acquired from the same lipid mixture containing 0.4% EqtII (PC/SM/EqtII mole ratio of 1000:100:4). One spectrum (Fig. 4 *b*) was acquired from the pellet collected after bench top centrifugation and one from the supernatant (Fig. 4 *c*). The spectrum from the pellet had a shape very similar to that of the spectrum of Fig. 4 *a* with both resonances slightly shifted upfield to −0.74 ppm for PC and to −0.13 ppm for SM, respectively. A similar upfield shift has been observed after membrane association of peptides and reflects subtle changes in the membrane surface charge density (Bonev et al., 2001b). A single line of low intensity and a chemical shift of 0.16 ppm was observed in the ^{31}P MAS NMR spectrum from the supernatant (Fig. 4 *c*). This most probably originates from small toxin-rich, and possibly SM-enriched, vesicles that were also observed in the electron micrographs and in the minor isotropic spectral component of the wideline ^{31}P and ^{2}H NMR spectra. This is in agreement with the relatively low intensity of the ^{31}P MAS NMR line compared to the total spectral intensity from the bilayer phospholipids from the pellet (Fig. 4 *b*).

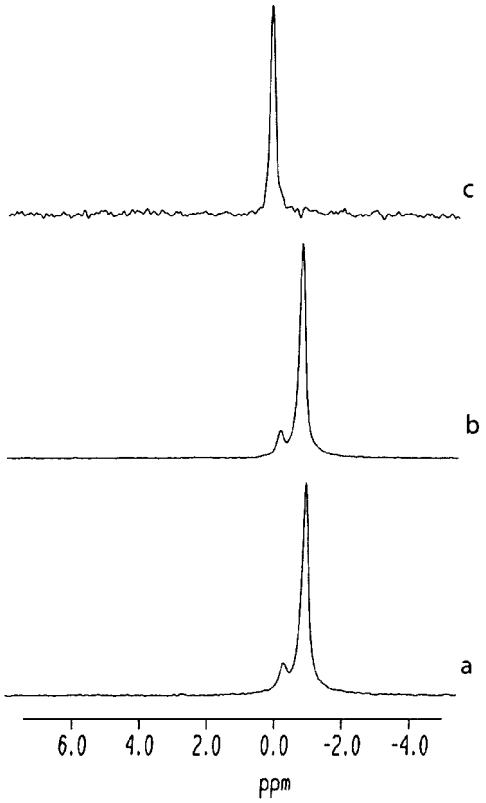

FIGURE 4 Phosphorus-31 MAS NMR at 40°C and 12 kHz spinning speed (500 MHz proton frequency) spectra from DMPC/SM mixtures in a MLV suspension: DMPC/SM (10:1 mol ratio) (*a*), and DMPC/SM /EqtII (1000:100:4 mol ratio) following 20 min benchtop centrifugation to produce a pellet (*b*), and supernatant (*c*).

Variable temperature ^{31}P MAS NMR

The temperature dependence of ^{31}P MAS longitudinal relaxation times in pure and mixed lipid bilayers with and without EqtII was investigated between 20°C and 50°C at 200 MHz proton frequency (81 MHz Larmor frequency for ^{31}P). The ^{31}P spin-lattice relaxation times, T_1, of each bilayer phospholipid constituent were determined simultaneously from the high resolution MAS NMR spectra. As the temperature was varied between 20°C and 50°C, T_1 increased from 1.1 to 1.6 s (Table 2) in pure DMPC bilayers (Fig. 5, *solid diamonds*), which suggests that the principal mode of lipid motions is in the fast regime. The small temperature variation of T_1 indicates the proximity to a T_1 minimum, which agrees with earlier relaxation measurements in mixed PC bilayers (Seelig, 1978; Milburn and Jeffrey, 1987). At 20°C, just below the phase transition, T_1 increases, leaving a discontinuous change, possibly, into a slow motions regime. This is the case for SM bilayers, as well, where the T_1 discontinuity is observed around 40°C, near the gel-fluid phase transition temperature (Fig. 5, *solid squares*). The ^{31}P T_1 takes a minimal value of 1.1 s between 40°C and 45°C and increases from 1.5 to 1.8 s as the

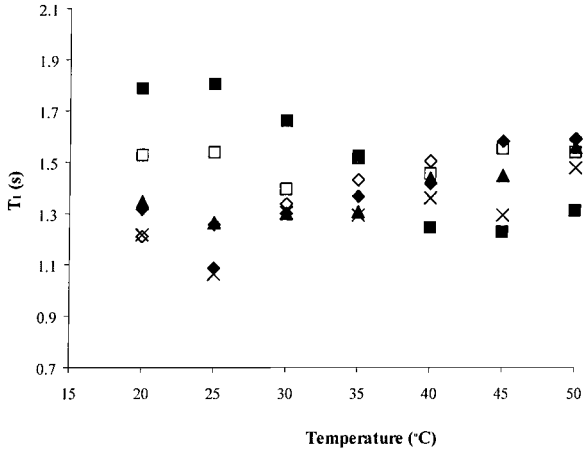

FIGURE 5 Phosphorus-31 longitudinal relaxation time, T_1, as a function of temperature recorded at 81 MHz from DMPC bilayers (♦), SM bilayers (■), PC in 1000 DMPC: 100 SM bilayers (▲), PC in 1000 DMPC: 4 EqtII bilayer mixtures (◇), PC in 1000 DMPC: 100 SM: 4 EqtII bilayer mixtures (×) and SM in 1000 DMPC: 100 SM: 4 EqtII bilayer mixtures (□). The acquisition parameters are described in Materials and Methods.

temperature is lowered from 35°C to 20°C into the gel phase, which suggests that the molecular dynamics of SM is slightly slower than that of DMPC.

The individual lipid components in a mixed lipid bilayer of 10:1 molar ratio DMPC/SM could not be resolved in the MAS NMR spectrum. The overall T_1 and its variation with temperature followed closely those of pure DMPC, which is expected from the large fraction of this lipid in the mixture (Fig. 5, *solid triangles*) and shows no specific perturbation of the DMPC dynamics by SM.

The longitudinal relaxation times from DMPC bilayers in the presence of 0.1 mol % EqtII were also very similar to those from the pure lipid. At higher temperatures a small decrease in T_1 was observed, compared to that from pure DMPC, suggesting a possible shift in the T_1 minimum toward a higher temperature and, therefore, lower rates of lipid motions in the presence of the toxin. This apparent contradiction with the decrease observed by ^{2}H NMR in the acyl chain orientational order may reflect a direct interaction between EqtII and the hydrophobic interior of the bilayer, which increases the orientational disorder in the chain methylenes but otherwise hinders the axial reorientation of the DMPC molecules.

In the case of mixed PC/SM (10:1 molar ratio) lipid bilayers with 0.4 mol % EqtII the individual spectral contributions from the two lipids were well resolved. The relaxation behavior of DMPC was practically identical to that of pure DMPC bilayers. In contrast, the SM T_1 increased in comparison to pure SM bilayers in the fluid phase from ~1.2–1.5 s and showed very little variation over the entire temperature interval. It remained lower than the 1.8 s value, measures from gel SM bilayers. These changes in the relaxation behavior of the two lipids are consistent with the

TABLE 2 Phosphorus-31 MAS NMR longitudinal relaxation times, T_1, from pure and mixed lipid membranes with and without 0.4% EqtII as a function of temperature recorded at 81 MHz phosphorus Larmor frequency. All lipid ratios are mol:mol

	$T_1 \pm 0.03$ (s)						
Sample (mol:mol)	20°C	25°C	30°C	35°C	40°C	45°C	50°C
DMPC	1.3	1.1	1.3	1.4	1.4	1.6	1.6
SM	1.8	1.8	1.7	1.5	1.2	1.2	1.3
1000 DMPC: 100 SM	1.3	1.3	1.3	1.4	1.4	1.5	1.5
1000 DMPC: 4 EqtII	1.2	1.3	1.3	1.4	1.5	1.6	1.6
1000 DMPC: 100 SM: 4 EqtII (PC peak)	1.2	1.1	1.3	1.3	1.4	1.3	1.5
1000 DMPC: 100 SM: 4 EqtII(SM peak)	1.5	1.5	1.4	1.5	1.5	1.5	1.5

presence of proteolipid EqtII/SM complexes within the lipid bilayer, surrounded by a DMPC-rich fluid matrix. The SM mobility is much reduced in comparison to that in fluid SM membranes. A slight rise in the SM T_1 at lower temperatures reflects the excess SM, which may order around the proteolipid complexes.

Transverse relaxation

The ^{31}P spectra of hydrated lipid bilayers at 25°C (Fig. 1, *a–e*) indicate that the presence of either SM or EqtII causes a small change in lipid mobility and an increase in the observed isotropic line width. This is supported by magic angle spinning ^{31}P data (not shown), which show a decrease (by ~ 25%) in T_2 relaxation time from 3.7 ms to 2.7–2.8 ms when SM or EqtII is present (Table 1). This change is more pronounced when EqtII was added to samples containing SM. For the sample 1000 DMPC:100 SM:1 EqtII (Fig. 1 *d*), T_2 decreased further (by approx. 30%) to 1.7 ms. When the EqtII concentration was increased (1000 DMPC:100 SM:4 EqtII, Fig. 1 *e*), a more dramatic change in line shape was observed and T_2 decreased to 1.1 ms (Table 1). This change in lipid mobility was also supported by a threefold change in the MAS NMR spectral line width. The ^{31}P spectrum (Fig. 1 *e*) shows a characteristic T_2 broadening and is indicative of a gel or $P_{\beta'}$ phase, as observed in DMPC-SM mixtures (Lentz et al., 1981).

The spectra, shown in Fig. 1, *a–d*, are typical of phospholipids in the fluid L_α phase, which is also reflected in the ^{31}P MAS NMR relaxation times (T_2 and T_1) reported in Table 1 and Fig. 5. The presence of EqtII decreased T_1 for the DMPC in fluid phase samples (Fig. 5) but there was little effect on T_2, which remained in the range 3.4–3.8 ms at the higher temperature (40°C, Table 1), similar to the value obtained for pure DMPC at 25°C (already in the fluid phase). The slight increase in ^{31}P T_2 of the 1000 DMPC:100 SM:4 EqtII system probably reflects a contribution from the isotropic phase. The decrease in T_1 at higher temperatures with EqtII in DMPC/SM dispersions is due to a more efficient relaxation mechanism on the MHz timescale, resulting from a reduction in the rates of high frequency (~ ns) motions in the fluid phase and consistent with an increase in low frequency motions when the toxin is present (Cornell et al., 1983).

DISCUSSION

EqtII, for which only a partial insertion into the bilayer has been demonstrated (Hong et al., 2002), is a potent cytolytic agent, which is active at nM concentrations (Anderluh and Macek, 2002). At concentrations of 0.1 and 0.4 mol %, EqtII had a similar effect on DMPC bilayers to that of the integral membrane peptide gramicidin at concentrations of 16 mol % (Cornell et al., 1988). However, the relative molecular weight of gramicidin A (1882) is approximately ten times lower than that of EqtII (~20 kDa). So even if we scale for EqtII molecular weight relative to gramicidin A, we observe a similar effect on lipid bilayers for EqtII but at an order of magnitude lower protein mass. Although gramicidin is fully incorporated into the lipid bilayer, it is unlikely that this would be the case for EqtII for which only partial insertion into the lipid membrane is expected (Hong et al., 2002). Similarly, melittin, a lytic peptide from bee venom, at much higher concentrations (10 mol %) than EqtII in DMPC bilayers produces an increase in low-frequency motions and bilayer disruption (Smith et al., 1992). In comparison to many known membrane-perturbing peptides (e.g. magainins, tachyplesins, melittin, etc.) (Matsuzaki, 1998; Bechinger, 1999), EqtII has a far more disruptive effect on lipid bilayers at much lower concentrations.

Although only part of the EqtII molecule is likely to penetrate the lipid bilayer, EqtII influences the dynamics of all lipid molecules, causing over 10% of the phospholipid (estimated from the ^{2}H isotropic component at 45°C) to form a separate phase. This isotropic spectral component can be attributed to the presence of small vesicles, which were observed by EM. Pure DMPC vesicles of 10-nm radius, as a result of their decreased density and size compared with extended MLV (Watts et al., 1978), would not spin down in a bench centrifuge (Cornell et al., 1982) of the type used for MLV sample preparation. Thus, the small structures resulting from the action of EqtII on the MLV suspension must be more dense than pure DMPC SUVs and rich in EqtII. These EqtII-enriched proteoliposomes occur only when SM is present in the target membrane and appear to be a consequence of the EqtII-induced changes in the lipid.

Features characteristic of fluid-phase bilayers were seen at 40°C in both ^{31}P and ^{2}H wideline NMR spectra. In the presence of 10% SM, addition of EqtII triggered the formation of an isotropic component, the spectral contribution of which increased with increasing temperature and toxin concentration (Figs. 1 and 2). The main transition temperature for hydrated deuterated DMPC bilayers is ~20°C (Bonev and Morrow, 1997), and T_m for SM is around 40°C (Marsh, 1990). Further addition of EqtII to the DMPC-SM

bilayer system resulted in a two-component ^{31}P NMR spectrum at 40°C (Fig. 1 *j*) where a broad isotropic line at ~0 ppm was superimposed onto the powder pattern of Fig. 1 *f*. A similar isotropic feature was also observed in the ^{2}H wideline NMR spectra, acquired under similar conditions. This feature at nearly 0 ppm reflects almost complete motional averaging of the effective ^{31}P CSA of the lipid phosphates and points to the possible formation of very small lipid structures (diameter < 100 nm). The presence of such small structures was verified by EM. The deuterium NMR spectra acquired at 40°C also showed an increased fraction of the isotropic spectral component (at zero quadrupole splitting) superimposed onto the powder pattern (Fig. 2 *j*), which emphasizes the role EqtII plays in the formation of the new lipid phase. Since the deuterium spectra are from the labeled DMPC, this new lipid phase is not composed of SM alone. Since the spectral features of the bilayer and the nonbilayer phases are well resolved, the phospholipids in the non-bilayer phase must be in slow exchange (exchange time > ms) with the prevailing bilayer phase.

The ^{31}P MAS longitudinal relaxation times of pure PC and pure SM bilayers showed a discontinuity across the lipid main transition (Fig. 5). Although T_1 of pure DMPC bilayers in the fluid phase remained almost unaffected by the addition of 0.4% toxin, the T_1 change across the lipid main transition disappeared. In contrast, addition of 0.4% EqtII to mixed DMPC:SM bilayers lead to a pronounced increase in SM T_1 from 1.2 to 1.5 s in the fluid phase and a somewhat smaller decrease in the PC T_1, from 1.5 to 1.4 s. The longitudinal relaxation of SM in a mixed lipid bilayer of 1000:100:4, PC:SM:EqtII remained essentially unaffected by temperature, whereas that of PC followed the temperature behavior of pure PC bilayers. This leads to a model where SM is preferentially engaged by the toxin into lateral proteolipid membrane domains, while PC exists in a lipid mixture, effectively segregated away from the protein within the bilayer.

In contrast to gradient centrifugation, which focuses the different lipid dispersions into isopicnic bands, the observation of phospholipid in the supernatant from DMPC:SM:EqtII (1000:100:4 mol ratio) after bench top centrifugation probably results from the gentle conditions during the precipitation process. This incomplete precipitation of the proteolipid suspension during sample preparation has prevented us from applying the quantitative analysis of the protein/lipid content, which was implemented for pneumolysin (Bonev et al., 2001a). In the latter case precipitation was facilitated by two additional factors—the presence of a toxin-induced lipid aggregation and the enormity of the pneumolysin oligomers (~3 MDa).

Two phenomena appear to take place in mixed PC/SM bilayers when EqtII is present at 0.1 to 0.4%. Firstly, we propose that a lateral phase separation occurs: the toxin appears to engage bilayer SM into lateral domains, enriched in this lipid, which are surrounded by SM-depleted DMPC bilayer phase. Such demixing, which can be inferred from the changes in the deuterium quadrupole splittings and ^{31}P effective CSA, as well as from the temperature dependence of ^{31}P T_1, may not require the disruption of the bilayer structures. Secondly, a true three-dimensional phase separation appears to be induced by EqtII, where the presence of toxin leads to the formation of highly curved, possibly bilayer structures, which are topologically disconnected from the bulk bilayer phase. Such phase would lead to the presence of an isotropic feature in the wideline ^{31}P and ^{2}H NMR spectra. It appears as a distinct resonance in the ^{31}P MAS NMR spectra at chemical shift, different from these of the bilayer lipids and is seen in the electron micrographs as small, possibly unilamellar, structures, budding off the bulk MLV lipid. The formation of small structures of similar nature has also been observed during the action of fusion peptides interacting with lipid bilayers (Agirre et al., 2000; Batista and Jezernik, 1992).

Caaveiro et al., (2001) have shown that EqtII is significantly more effective when inducing leakage in DMPC vesicles containing SM or cholesterol than in vesicles of pure DMPC. Cholesterol has an ordering effect on lipid bilayers (Lentz et al., 1981) and its role in enhancing the toxic action of EqtII is unclear. Some clues might be sought from the action of cholesterol-binding toxins, where cholesterol is proposed to mediate self-association of the toxin in the target membrane. The isotropic peak seen by both ^{31}P and ^{2}H NMR could be taken as evidence of bilayer disruption and/or membrane lysis.

EqtII, like other actinoporins, appears to recognize SM both at the level of the headgroup, as indicated by the fact that SM analogs with a modified phosphoric group are resistant to these toxins (Meinardi et al., 1995), and by the ceramide moiety because the ganglioside GM 1, with the same ceramide moiety as SM, could mimic its action (Macek et al., 1994). Lytic activity by EqtII requires the presence of SM in cell membranes (Belmonte et al., 1993; Macek et al., 1994) and the specific interaction of EqtII with SM warrants further investigation.

It has been suggested that other SM-preferring cytolysins, sticholysin I and II (Valcarcel et al., 2001), may form toroidal pores (Yang et al., 2000; Yang et al., 2001), which have been shown by neutron reflectivity (Gilbert et al., 1998), and by us using solid-state NMR and EM (Bonev et al., 2000b, 2001a) to occur during the action of the bacterial toxin pneumolysin. At the concentrations of EqtII used in this study, the toxin is likely to be predominantly in the monomeric state (Macek et al., 1995; Tejuca et al., 1996) and pores would not be the cause of the isotropic signal. The lipid-protein interaction that we describe here is more likely related to non-pore activity of the toxin, and no pores were observed in MLVs in our EM studies. Our NMR results show that in the presence of SM EqtII promotes formation of an isotropic lipid phase and slows down lipid mobility, and the EM data show the formation of small vesicles on the surface of MLVs as a consequence of

the toxin disrupting the mixed-lipid bilayers. The toxin in the remaining multilamellar structures appears to engage selectively SM into lateral proteolipid domains surrounded by PC-enriched lipid matrix. Further NMR studies of labeled EqtII in lipid bilayers are proposed in order to determine the location of the toxin in the membrane.

B.B. would like to thank Professor David Shotton for his advice on electron microscopy. G.A. kindly acknowledges Irena Pavesic for her excellent technical assistance. F.S. would like to thank Dr. Stuart Grieve for assistance with NMR spectral acquisition and Mr. Ben Atcliffe for the calorimetry and density gradient centrifugation.

Funding in part from the Higher Education Funding Council for England, the Medical Research Council, and the Biotechnology and Biological Sciences Research Council is gratefully acknowledged. A.W. is a BBSRC Professorial fellow.

REFERENCES

Agirre, A., C. Flach, F. M. Goni, R. Mendelsohn, J. M. Valpuesta, F. J. Wu, and J. L. Nieva. 2000. Interactions of the HIV-1 fusion peptide with large unilamellar vesicles and monolayers. A cryo-TEM and spectroscopic study. *Biochim. Biophys. Acta*. 1467:153–164.

Anderluh, G., A. Barlic, Z. Podlesek, P. Macek, J. Pungercar, F. Gubensek, M. L. Zecchini, M. D. Serra, and G. Menestrina. 1999. Cysteine-scanning mutagenesis of an eukaryotic pore-forming toxin from sea anemone: topology in lipid membranes. *Eur. J. Biochem*. 263:128–136.

Anderluh, G., and P. Macek. 2002. Cytolytic peptide and protein toxins from sea anemones (Anthozoa: *Actiniaria*). *Toxicon*. 40:111–124.

Anderluh, G., J. Pungercar, B. Strukelj, P. Macek, and F. Gubensek. 1996. Cloning, sequencing and expression of equinatoxin II. *Biochem. Biophys. Res. Commun*. 220:437–442.

Athanasiadis, A., G. Anderluh, P. Macek, and D. Turk. 2001. Crystal structure of the soluble form of Equinatoxin II, a pore-forming toxin from the sea anemone *Actinia equina. Structure*. 9:341–346.

Batista, U., and K. Jezernik. 1992. Morphological changes of V-79 cells after Equinatoxin II incubation. *Cell Biol. Int. Rep*. 16:115–123.

Bechinger, B. 1999. The structure, dynamics and orientation of antimicrobial peptides in membranes by multidimensional solid-state NMR spectroscopy. *Biochim. Biophys. Acta*. 1462:157–183.

Belmonte, G., G. Menestrina, C. Pederzolli, I. Krizaj, F. Gubensek, T. Turk, and P. Macek. 1994. Primary and secondary structure of a pore-forming toxin from the sea anemone, *Actinia equina* L., and its association with lipid vesicles. *Biochim. Biophys. Acta*. 1192:197–204.

Belmonte, G., C. Pederzolli, P. Macek, and G. Menestrina. 1993. Pore formation by the sea anemone cytolysin equinatoxin II in red blood cells and model lipid membranes. *J. Membr. Biol*. 131:11–22.

Bernheimer, A. W., and L. S. Avigad. 1976. Properties of a toxin from the sea anemone *Stoichactis helianthus*, including specific binding to sphingomyelin. *Proc. Natl. Acad. Sci. USA*. 73:467–471.

Bonev, B., R. C. J. Gilbert, P. W. Andrew, O. Byron, and A. Watts. 2001a. Structural analysis of the protein/lipid complexes associated with pore formation by the bacterial toxin pneumolysin. *J. Biol. Chem*. 276:5714–5719.

Bonev, B. B., A. Watts, M. Bokvist, and G. Gröbner. 2001b. Electrostatic peptide-lipid interactions of amyloid β-peptide and pentalysine with membrane surfaces monitored by ^{31}P MAS NMR. *Phys. Chem. Chem. Phys*. 3:2904–2910.

Bonev, B. B., W. C. Chan, B. W. Bycroft, G. C. K. Roberts, and A. Watts. 2000a. Interaction of the lantibiotic nisin with mixed lipid bilayers: A P-31 and H-2 NMR study. *Biochemistry*. 39:11425–11433.

Bonev, B., R. C. J. Gilbert, and A. Watts. 2000b. Structural investigation of pneumolysin / lipid complexes. *J. Membr. Biol*. 17:229–235.

Bonev, B. B., and M. R. Morrow. 1997. Effect of pressure on the dimyristoyl phosphatidyl choline bilayer main transition. Phys. Rev. E Stat. Phys. Plasmas Fluids Relat. Interdiscip. Topics. 55:5925–5833.

Bonev, B., and M. Morrow. 1996. Effect of hydrostatic pressure on bilayer phase behaviour and dynamics of dilauroylphosphatidylcholine. *Biophys. J*. 70:2727–2735.

Broekaert, W. F., B. P. A. Cammue, M. F. C. DeBolle, K. Thevissen, G. W. De Samblanx, and R. W. Osborn. 1997. Antimicrobial peptides from plants. *CRC Crit. Rev. Plant Sci*. 16:297–323.

Caaveiro, J. M. M., I. Echanbe, I. Gutierres-Aguirre, J. L. Nieva, J. L. R. Arrondo, and J. M. Gonzalez-Manas. 2001. Differential interaction of Equinatoxin II with model membranes in response to lipid composition. *Biophys. J*. 80:1343–1353.

Carbone, M. A., and P. M. Macdonald. 1996. Cardiotoxin II segregates phosphatidylglycerol from mixtures with phosphatidylcholine: ^{31}P and ^{2}H NMR spectroscopic evidence. *Biochemistry*. 35:3368–3378.

Cornell, B. A., G. C. Fletcher, J. Middlehurst, and F. Separovic. 1982. The lower limit to the size of small of small sonicated phospholipid vesicles. *Biochim. Biophys. Acta*. 690:15–19.

Cornell, B. A., R. G. Hiller, J. Raison, F. Separovic, R. Smith, J. C. Vary, and C. Morris. 1983. Biological membranes are rich in low frequency motion. *Biochim. Biophys. Acta*. 732:473–478.

Cornell, B. A., L. E. Weir, and F. Separovic. 1988. The effect of gramicidin A on phospholipid bilayers. *Eur. Biophys. J*. 16:113–119.

Davis, J. H., K. R. Jeffrey, M. Bloom, M. I. Valic, and T. P. Higgs. 1976. Quadrupolar echo deuteron magnetic resonance spectroscopy in ordered hydrocarbon chains. *Chem. Phys. Lett*. 42:390–393.

Dempsey, C. E. 1990. The actions of melittin on membranes. *Biochim. Biophys. Acta*. 1031:143–161.

Gouaux, E. 1997. Channel-forming toxins: tales of transformation. *Curr. Opin. Struct. Biol*. 7:566–573.

Gilbert, R. J. C., J. Rossjohn, M. W. Parker, R. K. Tweten, P. J. Morgan, T. J. Mitchell, N. Errington, A. J. Rowe, P. W. Andrew, and O. Byron. 1998. Self-interaction of pneumolysin, the pore-forming protein toxin of *Streptococcus pneumoniae*. *J. Mol. Biol*. 284:1223–1237.

Haeberlen, U., and J. S. Waugh. 1969. Spin-lattice relaxation in periodically perturbed systems. *Phys. Rev*. 185:420–429.

Hinds, M. G., W. Zhang, G. Anderluh, P. E. Hansen, and R. S. Norton. 2002. Solution structure of the eukaryotic pore-forming cytolysin equinatoxin II: implications for pore formation. *J. Mol. Biol*. 315: 1219–1229.

Homans, S. W. 1992. A Dictionary of Concepts in NMR, Clarendon Press, Oxford.

Hong, Q., K. Qutierrez, Z. Podlesek, P. Macek, D. Turk, J. M. Gonzales-Manas, J. H. Lakey, and G. Anderluh. 2002. Two-step membrane binding of Equinatoxin II, a pore-forming toxin from the sea anemone, involves an exposed aromatic cluster and a flexible helix. *J. Biol. Chem*. 277:41946–41924.

Lentz, B. R., M. Hoechli, and Y. Barenholz. 1981. Acyl chain order and lateral domain formation in mixed phosphatidylcholine-sphingomyelin multilamellar and unilamellar vesicles. *Biochemistry*. 20:6803–6809.

Macek, P., G. Belmonte, C. Pederzolli, and G. Menestrina. 1994. Mechanism of action of equinatoxin II, a cytolysin from the sea anemone *Actinia equina* L. belonging to the family of actinoporins. *Toxicology*. 87:205–227.

Macek, P., and D. Lebez. 1988. Isolation and characterization of three lethal and hemolytic toxins from the sea anemone *Actinia equina* L. *Toxicon*. 26:441–451.

Macek, P., M. Zecchini, C. Pederzolli, M. Dalla Serra, and G. Menestrina. 1995. Intrinsic tryptophan fluorescence of equinatoxin II, a pore- forming polypeptide from the sea anemone *Actinia equina* L, monitors its interaction with lipid membranes. *Eur. J. Biochem*. 234:329–335.

Marsh, D. 1990. CRC Handbook of Lipid Bilayers, CRC Press, Inc., Boca Raton, FL.

Matsuzaki, K. 1998. Magainins as paradigm for the mode of action of pore forming peptides. *Biochim. Biophys. Acta*. 1376:391–400.

Meinardi, E., M. Florin-Christensen, G. Paratcha, J. M. Azcurra, and J. Florin-Christensen. 1995. The molecular basis of the self/non-self selectivity of a coelenterate toxin. *Biochem. Biophys. Res. Commun.* 216: 348–354.

Menestrina, G., G. Schiavo, and C. Montecucco. 1994. Molecular mechanism of action of bacterial toxins. *Mol. Aspects Med.* 15:79–193.

Michaels, D. W. 1979. Membrane damage by a toxin from the sea anemone *Stoichactis helianthus*. I. Formation of transmembrane channels in lipid bilayers. *Biochim. Biophys. Acta.* 555:67–78.

Milburn, M. P., and K. R. Jeffrey. 1987. Dynamics of the phosphate group in phospholipid bilayers. *Biophys. J.* 52:791–799.

Minn, A. J., P. Velez, S. L. Schendel, H. Liang, S. W. Muchmore, S. W. Fesik, M. Fill, and C. B. Thompson. 1997. Bcl-x_L forms an ion channel in synthetic lipid membranes. *Nature.* 385:353–357.

Pinheiro, T. J. T., and A. Watts. 1994. Resolution of individual lipids in mixed phospholipid-membranes and specific lipid cytochrome-c interactions by magic-angle-spinning solid-state P-31 NMR. *Biochemistry.* 33:2459–2467.

Pungercar, J., G. Anderluh, P. Macek, F. Gubensek, and B. Strukelj. 1997. Sequence analysis of the cDNA encoding the precursor of equinatoxin V, a newly discovered hemolysin from the sea anemone *Actinia equina*. *Biochim. Biophys. Acta.* 1341:105–107.

Seelig, J. 1977. Deuterium magnetic resonance: theory and application to lipid membranes. *Q. Rev. Biophys.* 10:353–418.

Seelig, J. 1978. ^{31}P nuclear magnetic resonance and the head group structure of phospholipids in membranes. *Biochim. Biophys. Acta.* 515: 105–140.

Severs, N. J., T. M. Newman, and D. M. Shotton. 1995. A practical introduction to rapid freezing techniques. *In* Rapid Freezing, Freeze-fracture and Deep Etching. Severs, N. J. and Shotton, D. M. editors. Wiley-Liss, New York. 31–50.

Shotton, D. M., and N. J. Severs. 1995. An introduction to freeze fracture and deep etching. *In* Rapid Freezing, Freeze-fracture and Deep Etching. N. J. Severs and D. M. Shotton, D. M., editors. Wiley-Liss, New York. 1–30.

Simpson, R. J., G. E. Reid, R. L. Moritz, C. Morton, and R. S. Norton. 1990. Complete amino acid sequence of tenebrosin-C, a cardiac stimulatory and haemolytic protein from the sea anemone *Actinia tenebrosa*. *Eur. J. Biochem.* 190:319–328.

Smith, R., F. Separovic, F. C. Bennett, and B. A. Cornell. 1992. Melittin-induced changes in lipid multilayers: a solid-state NMR study. *Biophys. J.* 63:469–474.

Tejuca, M., M. Dalla Serra, M. Ferreras, M. E. Lanio, and G. Menestrina. 1996. Mechanism of membrane permeabilization by sticholysin I, a cytolysin isolated from the venom of the sea anemone *Stichodactyla helianthus*. *Biochemistry.* 35:14947–14957.

Valcarcel, C. A., M. Dalla Serra, C. Potrich, I. Bernhart, M. Tejuca, D. Martinez, F. Pazos, M. E. Lanio, and G. Menestrina. 2001. Effects of lipid composition on membrane permeabilization by sticholysin I and II, two cytolysins of the sea anemone *Stichodactyla helianthus*. *Biophys. J.* 80:2761–2774.

Varanda, W., and A. Finkelstein. 1980. Ion and nonelectrolyte permeability properties of channels formed in planar lipid bilayer membranes by the cytolytic toxin from the sea anemone, *Stoichactis helianthus*. *J. Membr. Biol.* 55:203–211.

Watts, A., D. Marsh, and P. F. Knowles. 1978. Characterization of DMPC vesicles and their dimensional changes through the phase transition—-Molecular control of membrane morphology. *Biochemistry.* 17:1792–1801.

Yang, L., T. A. Harroun, T. M. Weiss, L. Ding, and H. W. Huang. 2001. Barrel-stave model or toroidal model? A case study on melittin pores. *Biophys. J.* 81:1475–1485.

Yang, L., T. M. Weiss, R. I. Lehrer, and H. W. Huang. 2000. Crystallization of antimicrobial pores in membranes: magainin and protegrin. *Biophys. J.* 79:2002–2009.

Zhang, W., M. G. Hinds, G. Anderluh, P. E. Hansen, and R. S. Norton. 2000. Sequence-specific resonance assignments of the potent cytolysin equinatoxin II. *J. Biomol. NMR.* 18:281–282.

Zorec, R., M. Tester, P. Macek, and W. T. Mason. 1990. Cytotoxicity of equinatoxin II from the sea anemone *Actinia equina* involves ion channel formation and an increase in intracellular calcium activity. *J. Membr. Biol.* 118:243–249.